(4)

David Taylor Research Center

Bethesda, Maryland 20084-5000

DTRC/CMLD-89/07 July 1989

Computation, Mathematics and Logistics Department
Research and Development Report

A Mechanical Power Flow Capability for the Finite Element Code NASTRAN

by

Stephen A. Hambric

Approved for public release; distribution unlimited.

MAJOR DTRC TECHNICAL COMPONENTS

CODE 011 DIRECTOR OF TECHNOLOGY, PLANS AND ASSESSMENT

12 SHIP SYSTEMS INTEGRATION DEPARTMENT

14 SHIP ELECTROMAGNETIC SIGNATURES DEPARTMENT

15 SHIP HYDROMECHANICS DEPARTMENT

16 AVIATION DEPARTMENT

17 SHIP STRUCTURES AND PROTECTION DEPARTMENT

18 COMPUTATION, MATHEMATICS & LOGISTICS DEPARTMENT

19 SHIP ACOUSTICS DEPARTMENT

27 PROPULSION AND AUXILIARY SYSTEMS DEPARTMENT

28 SHIP MATERIALS ENGINEERING DEPARTMENT

DTRC ISSUES THREE TYPES OF REPORTS:

1. **DTRC reports, a formal series,** contain information of permanent technical value. They carry a consecutive numerical identification regardless of their classification or the originating department.

2. **Departmental reports, a semiformal series,** contain information of a preliminary, temporary, or proprietary nature or of limited interest or significance. They carry a departmental alphanumerical identification.

3. **Technical memoranda, an informal series,** contain technical documentation of limited use and interest. They are primarily working papers intended for internal use. They carry an identifying number which indicates their type and the numerical code of the originating department. Any distribution outside DTRC must be approved by the head of the originating department on a case-by-case basis.

UNCLASSIFIED

SECURITY CLASSIFICATION OF THIS PAGE

REPORT DOCUMENTATION PAGE

1a REPORT SECURITY CLASSIFICATION UNCLASSIFIED	1b. RESTRICTIVE MARKINGS
2a SECURITY CLASSIFICATION AUTHORITY	3 DISTRIBUTION/AVAILABILITY OF REPORT Approved for public release; distribution unlimited
2b DECLASSIFICATION/DOWNGRADING SCHEDULE	
4 PERFORMING ORGANIZATION REPORT NUMBER(S) CMLD-89/07	5. MONITORING ORGANIZATION REPORT NUMBER(S)
6a NAME OF PERFORMING ORGANIZATION David Taylor Research Center 6b OFFICE SYMBOL (If applicable) Code 1844	7a. NAME OF MONITORING ORGANIZATION
6c ADDRESS (City, State, and ZIP Code) Bethesda, MD 20084-5000	7b. ADDRESS (City, State, and ZIP Code)
8a NAME OF FUNDING/SPONSORING ORGANIZATION Office of Naval Technology 8b. OFFICE SYMBOL (If applicable) ONT	9. PROCUREMENT INSTRUMENT IDENTIFICATION NUMBER
8c ADDRESS (City, State, and ZIP Code) 800 N. Quincy Street Arlington, VA 22217	10 SOURCE OF FUNDING NUMBERS PROGRAM ELEMENT NO. 62323N; PROJECT NO.; TASK NO. R2320; WORK UNIT ACCESSION NO. 1-1903-001

11 TITLE (Include Security Classification)

12 PERSONAL AUTHOR(S)
Stephen A. Hambric

13a TYPE OF REPORT	13b TIME COVERED FROM ____ TO ____	14. DATE OF REPORT (Year, Month, Day)	15. PAGE COUNT
		1989, July	32

16 SUPPLEMENTARY NOTATION

17 COSATI CODES		
FIELD	GROUP	SUB-GROUP

18. SUBJECT TERMS (Continue on reverse if necessary and identify by block number)
Power flow Mechanical Intensity
Finite Element Method
Structural Dynamics

19 ABSTRACT (Continue on reverse if necessary and identify by block number)

The identification of power flow paths in dynamically loaded structures is an important, but currently unavailable, capability for the finite element analyst. For this reason, methods for calculating power flows and mechanical intensities in finite element models are developed here. Formulations for calculating input and output powers, power flows, mechanical intensities, and power dissipations for beam, plate, and solid element types are derived. NASTRAN is used to calculate the required velocity, force, and stress results of an analysis, which a post-processor then uses to calculate power flow quantities. The SDRC I-deas Supertab module is used to view the final results. Test models include a simple truss and a beam-stiffened cantilever plate. Both test cases showed reasonable power flow fields over low to medium frequencies. Future work will include testing with more complex models, developing an interactive graphics program to view easily and efficiently the analysis results, applying shape optimization methods to the problem with power flow variables as design constraints, and adding the power flow capability to NASTRAN.

20 DISTRIBUTION/AVAILABILITY OF ABSTRACT	21. ABSTRACT SECURITY CLASSIFICATION
☒ UNCLASSIFIED/UNLIMITED ☐ SAME AS RPT ☐ DTIC USERS	UNCLASSIFIED
22a NAME OF RESPONSIBLE INDIVIDUAL Stephen A. Hambric	22b TELEPHONE (Include Area Code) (301)227-1645 22c. OFFICE SYMBOL

DD FORM 1473, 84 MAR 83 APR edition may be used until exhausted. All other editions are obsolete.

SECURITY CLASSIFICATION OF THIS PAGE
UNCLASSIFIED

CONTENTS

FIGURES

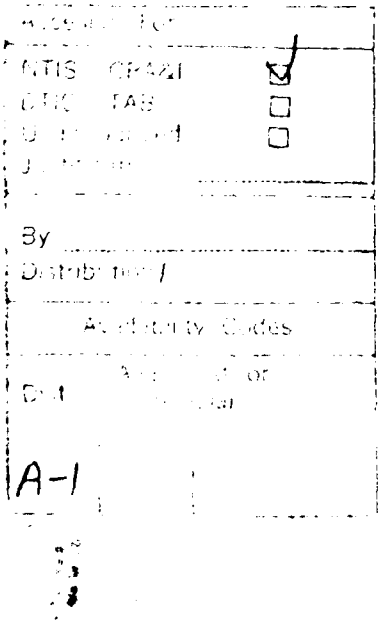

ABSTRACT

The identification of power flow paths in dynamically loaded structures is an important, but currently unavailable, capability for the finite element analyst. For this reason, methods for calculating power flows and mechanical intensities in finite element models are developed here. Formulations for calculating input and output powers, power flows, mechanical intensities, and power dissipations for beam, plate, and solid element types are derived. NASTRAN is used to calculate the required velocity, force, and stress results of an analysis, which a post-processor then uses to calculate power flow quantities. The SDRC I-deas Supertab module is used to view the final results. Test models include a simple truss and a beam-stiffened cantilever plate. Both test cases showed reasonable power flow fields over low to medium frequencies. Future work will include testing with more complex models, developing an interactive graphics program to view easily and efficiently the analysis results, applying shape optimization methods to the problem with power flow variables as design constraints, and adding the power flow capability to NASTRAN.

ADMINISTRATIVE INFORMATION

This work was performed under Program Element 62323N, Task Area R2320, Acoustic Silencing Task (Auxiliary Systems), and Work Unit 1-1903-001-10. The DTRC project managers were D.E. Goldsmith and L.T. Ho, DTRC Code 274.

INTRODUCTION

Structure-borne sound is the vibrational energy which travels through dynamically loaded mechanical systems. This vibrational energy is radiated eventually into an acoustic medium as noise. An example cited by Wohlever and Bernhard[1] is an airplane wing loaded by engine vibrations. The vibrational energy travels along the wing to the fuselage and is radiated as sound into the cabin. Architects face the problem of structure-borne sound in hotels and apartment buildings, where vibrational energy flows through walls and floors and is radiated as sound into other rooms. This problem is addressed by Luzzato and Ortola.[2]

Dynamic analyses performed to solve these problems produce large amounts of data. The analyst is then faced with the problem of interpreting the output. Tabular printouts, spectrum plots, and deformed shape plots are all useful ways of defining the state of a structure. Another way of quantifying the propagation of structure-borne sound is the calculation of power flows.

This method identifies the magnitude and direction of the power at any location in a structure and helps an analyst find the dominant paths of energy flow and the energy sinks in a given problem. Understanding the paths of energy which flow from a vibration source to other parts of a structure helps an engineer to pinpoint and correct vibration problems.

For naval applications, such as machinery in submarines and surface ships, quantifying power flow paths could lead to reduction of noise. Applying isolators and/or active control devices to a machinery system could reduce power flows along particular paths (to the hull for example) and therefore also reduce sound radiation.

The following important terms are used in this study: power flow, which is actually power or energy flow but is termed power flow by the scientific community of this field; mechanical intensity, which is power flow per unit area; and power dissipation, which is the time rate of energy dissipation in a structure.

Four main methods for identifying dominant power sources and power flow paths are addressed in the literature: experimental methods, statistical energy analysis, the finite element method, and a finite element analogy using heat conduction equations. Experimental solutions are the most common. The authors of some of these papers[3–7] use multiple transducers and digital signal processing techniques to solve various power flow problems. A common method is the calculation of cross spectral densities, in which two accelerometers are placed a known distance apart on a structure, and response spectra are generated for the two measurement locations. The spectra are statistically analyzed, and power flows are computed over some range of frequencies. This approach is similar to the two-microphone technique used by acousticians to solve noise propagation problems in fluid media. Once an experimental apparatus is set up, the analyst may easily vary applied loads and loading frequencies. Unfortunately, the added weights and inertias of the transducers attached to an experimental structure may produce accuracy problems.

Statistical energy analysis (SEA) is a computational method used to solve energy flow problems in the high frequency domain. A definitive reference on SEA is the text by R.L. Lyon.[8] In the SEA method, large structures are split into smaller subsystems; a modal density is estimated for each subsystem so the number of modes in a given frequency band can be determined; dissipation loss factors, which relate energy stored to power dissipated, are estimated for the subsystems; and coupling loss factors, which relate differences of modal energy of subsystems to power flow, are assigned to the junctions of the subsystems. The energy distribution, power flows, and power dissipations are then computed.

SEA is a good way of solving for the average response of structures at high frequencies; however, all spatial variations of the power flow field in the

substructures remain unknown. A more discrete method must be used to identify specific power flow paths through a structure. Finite element analysis (FEA) may be used for this purpose, but is cost effective only for low to mid-range frequencies, since higher mode shapes are more complex, wavelengths are shorter, and denser finite element meshes are required to model a problem correctly. Mickol and Bernhard[9] succesfully used FEA to identify power flow paths in simple beam and plate structures excited at low frequencies.

Recently, some scientists have proposed a new method to solve for power flows in the middle frequency range. Cuschieri,[10] Nefske and Sung,[11] and Wohlever and Bernhard[1] have been studying this new approach: a finite element analogy in which powers are substituted into a heat conduction equation and the power flow field is found directly.

In this paper FEA is used to solve the power flow problem. For lower modes the method is accurate, models are simple to build and modify using modern modeling software, and analysis results are viewed easily using post-processing graphics packages. Since we are not aware of any commercial software which contains a power flow capability, the formulations and computer methods are developed here for NASTRAN,[12] a widely used program for structural dynamics. The FEA studies presented in other literature consider only the contribution of flexural wave motion to power flow. Other motion types of power flow, such as axial and torsional, are ignored. In this study, all types of power flow are considered.

First, general methods and formulations for power flows, mechanical intensities, power dissipations, input powers, and output powers are developed for global models, beam elements, plate elements, solid elements, and scalar elements. The required NASTRAN solution, the algorithm of the power flow processor, and the use of I-deas Supertab (for post-processing and graphics) are outlined. Two test models are analyzed to verify the methods: a simple truss and a beam-stiffened cantilever plate. Finally, conclusions about the method are drawn from results of the test case analyses, and some thoughts about future directions for work are discussed.

THE FINITE ELEMENT SOLUTION

General Methods

A typical power flow cycle is shown in Fig. 1. The figure shows an arbitrary structure mounted to a connecting structure by a spring and damper coupling. A dynamic load is applied, and energy flows into the structure at the load point. The input power then flows through the structure along multiple flow paths denoted by arrows whose lengths represent power flow magnitudes. As the energy flows toward the mounting, it is dissipated by material damping and sound radiation into a surrounding medium, and the flow arrows shorten. The flow and dissipation processes continue until the remaining energy exits the structure through the mounting and flows into the connecting structure.

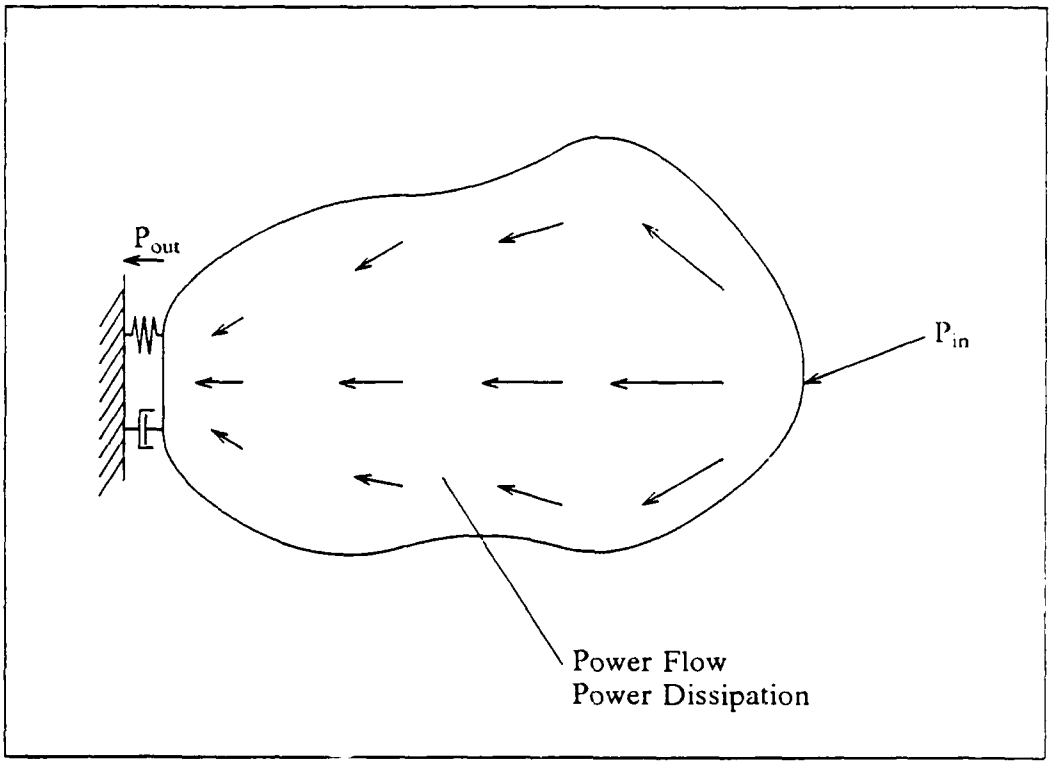

Fig. 1. Sample Power Flow Diagram.

Though only one power entry point and one exit point are shown in this drawing, multiple loads and mountings may exist. A classic text which describes the flow of structure-borne sound is the book by Cremer, Heckl, and Ungar.[13]

The structural dynamics problem may be solved using NASTRAN. The structure may be modeled with various element types; mountings are modeled with scalar spring, damping, and mass elements. Constraints and loads are directly applied. The steady-state response for the model is solved for a given excitation frequency, and the power flow variables are calculated.

Power Flow and Mechanical Intensity

Power is defined as the time averaged product of a force with the in-phase component of velocity in the direction of the force. For time-harmonic analysis, where complex numbers are used, this calculation may be visualized as taking the dot product of the force and velocity phasors.

Multiplying one complex number by the in-phase part of another complex number is the same operation as multiplying the first number by the

complex conjugate of the other number and taking the real part of the result. Therefore a general formula for power flow in a structure is

$$\text{Power} = \text{Real}\,[\vec{F}\,\vec{v}^{\,*}], \tag{1}$$

where

$\vec{F}$ = force vector and
$\vec{v}^{\,*}$ = complex conjugate of velocity vector.

The real part of power flow is called the active power.

Mechanical intensity is power flow per unit area, or stress (force per unit area) multiplied by the complex conjugate of velocity. Mechanical intensity is similar to acoustic intensity in a fluid medium, which is the product of pressure and the in-phase component of particle velocity.

Damping and Power Dissipation

Power may be dissipated in several ways: by material damping, by mountings and other passive and active devices, and by radiation as sound. This section discusses power dissipation due to damping. For now only material damping is considered in the dissipation process. The effects of sound radiation will be considered in the future.

Power dissipation is calculated differently from power flow and power input. Since power dissipation is the rate of energy dissipation, the energy level of a given element is calculated and multiplied by its damping coefficient. Multiplying the energy dissipation by the angular frequency of excitation gives the power dissipated in that element.

The effects of the material damping coefficient are significant. As the damping coefficient is increased, the power dissipated increases. If the damping coefficient is zero, no scalar damping elements are applied to the structure, and no sound radiation is considered, power dissipation will be zero and no power flow will exist. This is because, with no damping, forces and velocities will be exactly 90 degrees out of phase, and the in-phase part of velocity with force is zero. Although this situation is physically unrealistic, it may occur in a finite element analysis.

To solve for power dissipation, energy dissipation must first be calculated. The energy level in an element is the sum of the element's kinetic energy and potential energy. Since this is a steady-state problem, and the energy is a time-averaged quantity, it may be calculated as twice the kinetic energy:

$$E = mvv^{*}, \tag{2}$$

where

E = energy,
m = element mass, and

v = velocity.

Power dissipation is then calculated as

$$P_{diss} = 2\pi f \eta E, \tag{3}$$

where

f = rotational frequency, and
η = material damping coefficient.

The ηE term is the energy dissipation, and multiplying by the angular frequency gives the energy dissipation per unit time, or power dissipation. The result will be a real number, since the energy calculation multiplies velocity by its complex conjugate.

Eq. 3 is based on two assumptions: η is small (< 0.4), and f is a resonance frequency. The calculation of power dissipation is more complicated for off-resonance frequencies. For a one degree of freedom (DOF) system the equation for power dissipation is multiplied by ω_n/ω, where ω_n is the natural frequency and ω is the excitation frequency. For multi-DOF systems, such as finite element models, total power dissipation for a given frequency must be calculated as the sum of the contributions from each of the model's mode shapes. This requires a modal, rather than direct frequency response analysis. Although a modal solution would generate the data necessary for accurate power dissipations, error may be introduced to the power flow computations. Since the forces and velocities of a modal analysis are calculated as the sums of the contributions of the mode shapes, they may be inaccurate if an insufficient number of modes are used for the summation. At this point, power flows are considered the more important of the calculations and a direct frequency response analysis is performed. Therefore, only the power dissipations calculated at or near resonance frequencies are accurate using Eq. 3.

Since the calculation of power dissipation involves the element mass, the calculation is mesh-dependent. As mesh density increases, element power dissipations decrease. For example, if a beam element is subdivided into two beam elements, the original power dissipation is split between the two new beams. Power dissipation can be made independent of the mesh by dividing by element volumes, but at this point the actual power dissipations are calculated because of their importance in checking power balances (see the *Power Balance* section below).

Also, power dissipation is directly related to the mode shapes of an analysis, so areas of large displacements and velocities will be large energy sinks, and nodes (points of near zero displacement) will dissipate almost no power.

Power Input

Power inputs are calculated by multiplying input forces by the complex conjugates of the resulting velocities at the load points. Total input power is calculated as

$$P_{in} = \text{Real}\left[\sum_{i=1}^{n} F_i v_i^*\right], \tag{4}$$

where

i = load point, and
n = number of loads.

This is a global calculation which is independent of element type.

Presently, only force inputs are considered. Other load types applied to a finite element model such as displacements, velocities, and accelerations, may input power to a structure. The calculation of input powers for these load types will be derived in a subsequent paper.

Power Output

Power output is the power that leaves the system through its mountings and enters the connecting system(s). The external system is modeled using spring, damper, and mass elements. These scalar elements must be connected to additional grid points, which are grounded. The forces of constraint are combined with the velocities of the grid attached to the scalar element to calculate power output. The power output is calculated as

$$P_{out} = \text{Real}\left[\sum_{j=1}^{n} F_j v_j^*\right], \tag{5}$$

where

j = grounded grid, and
n = number of grounded grids.

Power Balance

The previously defined terms (power input, power dissipation, and power output) are all used to verify a power balance for a given problem. The power balance equation is

$$P_{in} = \sum_{k=1}^{\#elem} P_{diss} + P_{out}. \tag{6}$$

This same equation is used in SEA theory. Since P_{in}, P_{out}, and P_{diss} are all calculated independently, if the power balance equation holds, then the power flow solution is correct (assuming the original finite element solution is accurate). This power equilibrium equation is therefore an important check on the power formulations and calculations.

Element Formulations

Beam Elements

Much of the literature in the field of power flow is devoted to beams. Noiseux[14] and Verheij[15] described methods of measuring the flexural power flow in beams. Other authors, such as Li,[16] Wohlever and Bernhard,[1] and Nefske and Sung,[11] have developed power flow capabilities for beam elements.

All the methods developed, however, consider only flexural power flow. Though flexure is arguably the dominant response in a beam, axial and torsional response can also be important. For this reason, all possible components of power flow will be considered here.

Power flow methods for NASTRAN BAR element types are derived in this section. Either lumped mass or coupled mass solutions may be used. Unfortunately, torsional inertia for the BAR element type is not calculated by NASTRAN. Concentrated mass elements with beam torsional inertias entered as masses must be added to the model at the appropriate DOF to solve for accurate torsional power flows.

Power Flow and Mechanical Intensity. A diagram of the BAR element and its force output conventions is shown in Fig. 2, where plane 1 is vertical and plane 2 is horizontal. Since a beam is a one-dimensional element, energy flows in only one direction: in the local x direction, or along the length of the beam. The total power flow for a beam element is

$$P_x = \text{Real}\,[-(F_x v_x^* + V_1 v_y^* + V_2 v_z^* + T\dot{\theta}_x^* - M_2\dot{\theta}_y^* + M_1\dot{\theta}_z^*)], \tag{7}$$

where

F_x = axial force,
V_1 = shear force in y direction,
V_2 = shear force in z direction,
T = torsion about x,
M_2 = bending moment about y,
M_1 = bending moment about z,
v_i = translational velocities in direction i, and
$\dot{\theta}_i$ = rotational velocities about axis i.

The negative sign on the result comes from force and displacement direction conventions for the element. Negative signs appear in the formulations for the plate and solid elements for the same reason. The negative sign on the M_2 term reflects the NASTRAN force output convention. In Fig. 2, M_2 is shown as positive in the opposite sense to $\dot{\theta}_y$. Therefore, $M_2\dot{\theta}_y^*$ is opposite in sign to the other power flow components.

Velocities are calculated by NASTRAN for each grid point, and beam forces are calculated on an element level. This difference creates a problem, because some way of solving for a power flow on an element level is required.

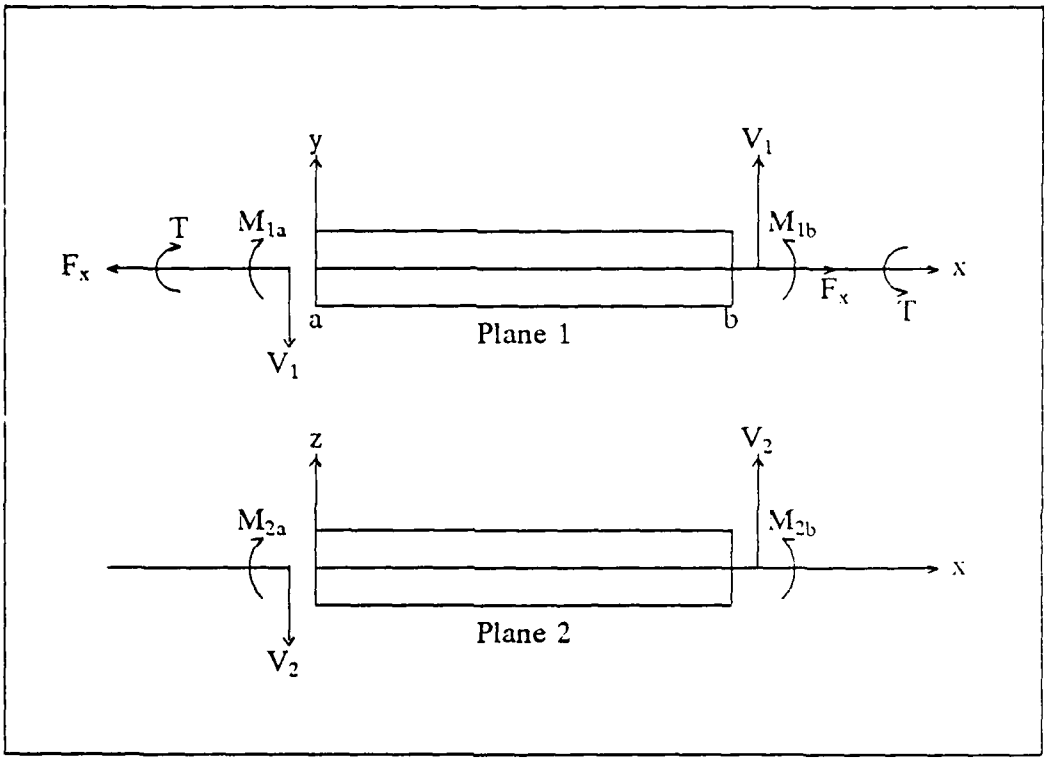

Fig. 2. The BAR Element

The solution is to solve for a power flow at each grid point and then calculate the average quantity for an element.

Shear, axial, and torsional forces are constant through the element and are the same for each grid point. Bending moments are calculated at each end of the beam element. Velocities are solved for at a global level, and a coordinate system transformation must be performed to find the velocities at the element level. Since the grid coordinates and beam orientation vector are given, the velocity transformation is straightforward. After power flows at each element end are calculated, they are averaged to give an element power flow. Power flows are then transformed back to NASTRAN's basic coordinate system.

Two important observations may be made about power flow in NASTRAN beam elements. Since power flow is one-dimensional in beams, it is independent of mesh variations. Increasing mesh density or varying the mesh pattern will not affect greatly the power flow results (assuming the mesh is dense enough to model accurately the wave shapes of the solution). Also, since power flow is dependent on element force quantities (axial and shear

forces, torsion) that are discrete values at each element, the power flow and mechanical intensity quantities are not continuous across beam element boundaries (from element to element).

Power Dissipation. The energy of a beam element includes both translational and rotatory terms, and is calculated as

$$E = m(v_x v_x^* + v_y v_y^* + v_z v_z^*) + I_{xx}\dot{\theta}_x\dot{\theta}_x^* + I_{yy}\dot{\theta}_y\dot{\theta}_y^* + I_{zz}\dot{\theta}_z\dot{\theta}_z^*, \quad (8)$$

where

m = element mass,
I_{yy}, I_{zz} = mass moments of inertia about cross section,
I_{xx} = polar mass moment of inertia about beam axis,
v_i = local translational velocities in direction i, and
$\dot{\theta}_i$ = local rotational velocities about axis i.

The element energy is multiplied by $2\pi\eta f\omega_n/\omega$, as in Eq. 3, to yield power dissipation. As mentioned earlier, the ω_n/ω term complicates the calculation so that only power dissipations at or near resonances will be accurate at this time.

The rotational inertial energies are generally small. However, if the beam lengths are long with respect to the cross section, the mass moments of inertia become important. In the case of torsion, where the only large displacement is rotation about the beam's axis, the polar mass moment of inertia term dominates the energy calculation.

Plate Elements

Many Naval structures require the use of plate elements to accurately model them. Since the beam element formulation included all components of power flow, power flow capabilities for quadrilateral plate elements, which consider both flexural and membrane effects, are developed.

The literature concerning plate elements is growing, and publications by Mickol and Bernhard,[9] Williams et al,[17] Koshiroi and Tateishi,[18] Noiseux,[14] Fahy and Pierri,[19] and Cuschieri,[20] investigate mechanical intensities and power flows through plate structures. As with the literature for beams, however, most approaches consider only flexural effects.

Power Flow and Mechanical Intensity. A diagram of a QUAD element and its force and stress output conventions is shown in Fig. 3. The quadrilateral element is two-dimensional, and power may flow in the local x and y directions. The power flow in the x direction is calculated as

$$P_x = \text{Real}\,[-(V_x v_z^* - M_x\dot{\theta}_y^* + M_{xy}\dot{\theta}_x^* + F_x v_x^* + F_{xy} v_y^*)]; \quad (9)$$

the power flow in the y direction is

$$P_y = \text{Real}\,[-(V_y v_z^* + M_y\dot{\theta}_x^* - M_{xy}\dot{\theta}_y^* + F_y v_y^* + F_{yx} v_x^*)],$$

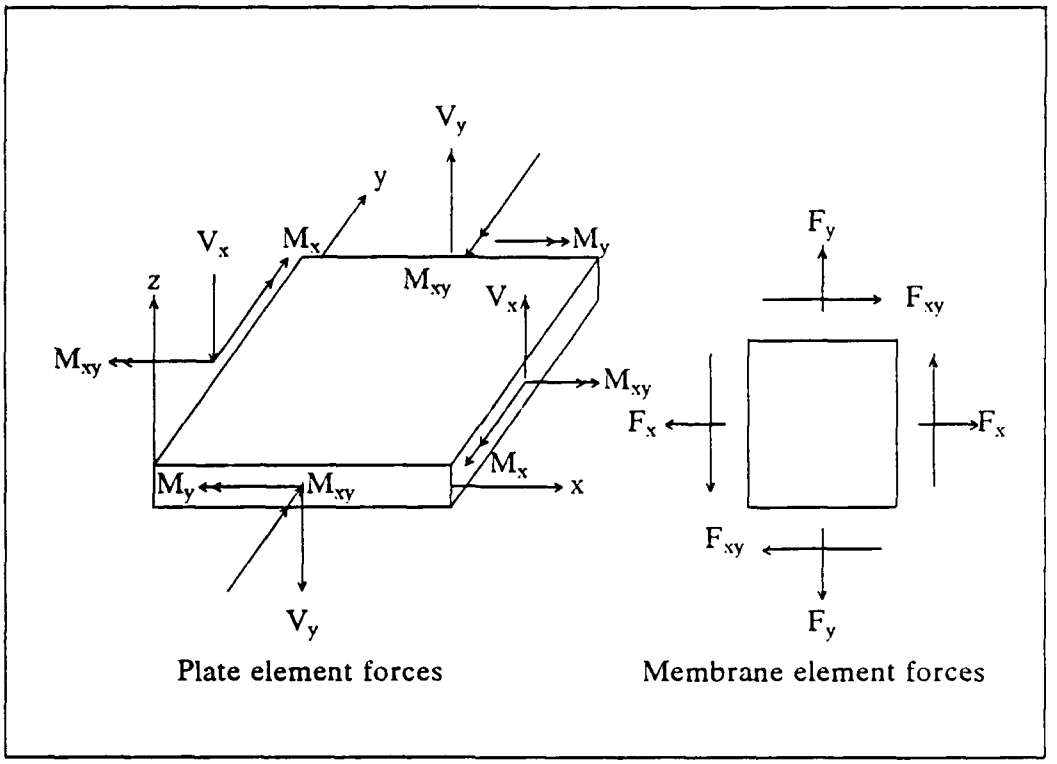

Fig. 3. The QUAD Element

where

V_x, V_y = transverse shear forces,
M_x, M_y = bending moments,
M_{xy} = twisting moment about x and y,
F_x, F_y = membrane forces,
F_{xy}, F_{yx} = membrane shear,
v_i = local translational velocities in direction i, and
$\dot{\theta}_i$ = local rotational velocities about axis i.

The negative signs on the $M_x\dot{\theta}_y^*$ and $M_{xy}\dot{\theta}_y^*$ terms conform to the NASTRAN force output convention. These bending moments are opposite in sense to their corresponding rotational velocities. All forces, both flexural and membrane, are per unit width. Therefore the units for power flows in QUAD elements are power per unit length.

As was the case for beam elements, grid velocities here must be transformed to the local element coordinate systems to be used in the power

flow calculations. After the calculations, the power flow vectors are transformed back to NASTRAN's basic coordinate system.

Since the quantities used to calculate power flows for plate elements (forces per unit width and velocities) are both mesh independent, power flow per unit length is also mesh independent. To solve for mechanical intensities, power flow is divided by plate thickness, giving power per unit area. Mechanical intensities for QUADs are also mesh independent.

Power Dissipation. The energy of a QUAD element, when only scalar mass terms are considered, is

$$E = m(v_x v_x^* + v_y v_y^* + v_z v_z^*), \tag{10}$$

where

m = element mass, and
v_i = local translational velocities in direction i.

Element energies are multiplied by $2\pi\eta f\omega_n/\omega$ to calculate power dissipations. Power dissipation terms are calculated at each grid point and averaged to solve for the element dissipation. This calculation is mesh-dependent, since power dissipation is directly related to element mass. The same difficulties that applied to BAR elements due to the ω_n/ω term apply for QUAD elements.

Solid Elements

Since literature in the power flow field comes largely from the experimental sector, solid elements are generally not considered. An experimentalist cannot place a measuring device inside the material of a solid structure. The paper by Pavic,[7] however, describes a method for measuring structural surface intensity. His method, which involves placing transducers on various surfaces of a machinery system to measure two-dimensional mechanical intensities, may be extended to three dimensions. Since a finite element code has no restrictions on making "measurements" internal to a structure, mechanical intensities may be calculated throughout a solid model.

Power Flow and Mechanical Intensity. For the BAR and QUAD elements, force output is provided by NASTRAN. For solid elements (isoparametric IHEXi element types), stress output is solved for at grid points and at the element centroids. Pavic[7] uses stresses and velocities in his formulation of structural surface intensities. His formulas for mechanical intensities, extended to three dimensions, are

$$I_x = \text{Real}\,[-(\sigma_x v_x^* + \tau_{xy} v_y^* + \tau_{xz} v_z^*)], \tag{11}$$

$$I_y = \text{Real}\,[-(\sigma_y v_y^* + \tau_{yx} v_x^* + \tau_{yz} v_z^*)],$$

$$I_z = \text{Real}\,[-(\sigma_z v_z^* + \tau_{zx} v_x^* + \tau_{zy} v_y^*)],$$

where

I_x, I_y, I_z = global mechanical intensities,
$\sigma_x, \sigma_y, \sigma_z$ = normal stresses,
$\tau_{xy}, \tau_{yz}, \tau_{xz}$ = shear stresses, and
v_i = global translational velocities in direction i.

Since element stresses are given in the basic coordinate system, the velocities do not have to be transformed to element coordinate systems as they were for the BAR and QUAD element types. Calculations are made at each grid point and averaged to calculate the element mechanical intensity.

Since the quantities used to calculate mechanical intensities for solid elements (stresses and velocities) are both mesh independent, the mechanical intensities are also mesh independent.

Power Dissipation. The power dissipation calculations are similar to those for the QUAD elements (Eq. 10). Only mass and translational velocity terms are considered. Power dissipation terms are calculated at each grid point and averaged. Again, since the element mass is directly related to the element energy, power dissipation is mesh-dependent. Also, the ω_n/ω term in the calculation is a problem for solids as well as for beams and plates.

Scalar Elements

Scalar elements may be used to simulate mountings and structures connected to the finite element model. Scalar springs, dampers, and masses may be used to model stiffness, damping, and mass effects. These elements may be important for certain analyses, such as those for a structure not rigidly mounted. In certain cases, power may flow out of a structure into an isolator, which will absorb much of the energy, or into a surrounding medium. The accurate modeling of boundary conditions must therefore include scalar element types.

Power flows and power dissipations are not yet computed in scalar elements, but the presence of external stiffnesses, dampers, and masses may significantly affect the results in the structural element types.

Computer Methods

A flow chart of the solution process is shown in Fig. 4. NASTRAN's Rigid Format 8 (Direct Frequency Response) is used to solve problems for any combination of load cases and excitation frequencies. The model information

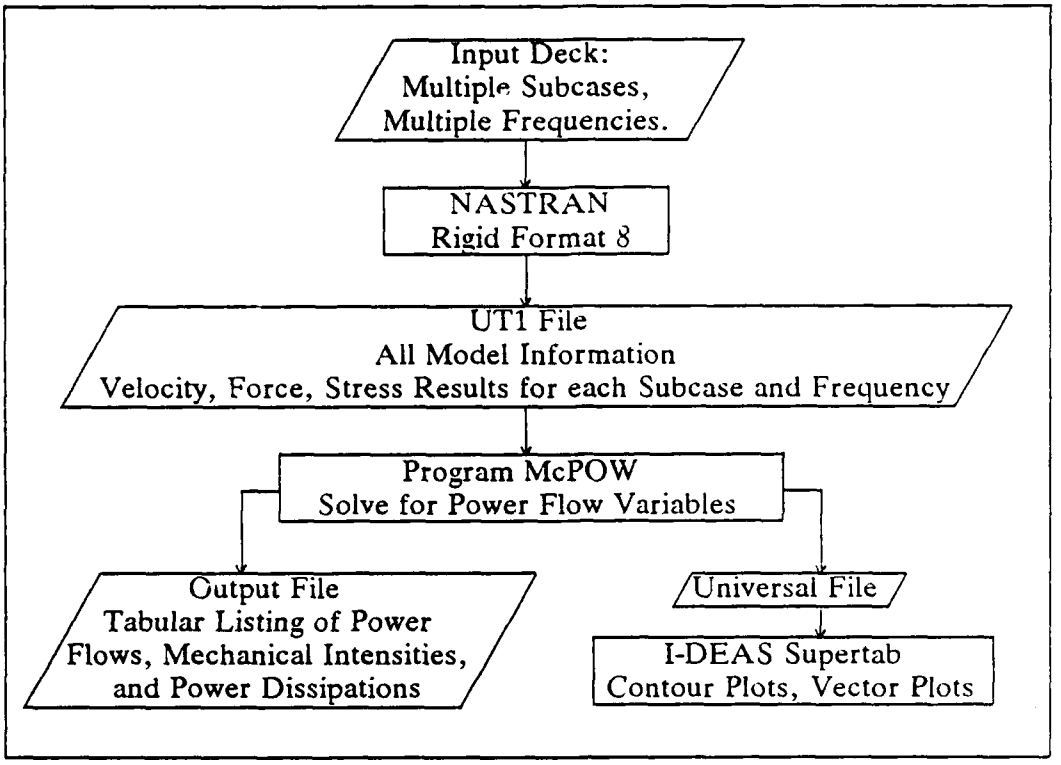

Fig. 4. Power Flow Solution Process

and problem solution output are written on a UT1 file, which is used as input to the McPOW (Mechanical POWer) program. After the power computations have been made, power flows, mechanical intensities, and power dissipations are written on two output files. One file contains a tabular listing of the power flow results; the other file is formatted as input to the I-DEAS Supertab[21] post-processor, which is used to interpret visually the results.

NASTRAN Solution

Before Rigid Format 8 is run, an eigenvalue extraction (Rigid Format 3) can be performed on the model to determine the resonant frequencies and their corresponding mode shapes. Power flows can then be measured at response peaks, and the dominant type of power flow, such as flexural or axial, can be predicted by examining the mode shapes.

Power Flow Algorithm

The program McPOW is composed of four main sections: the model information section, the NASTRAN output section, the power flow calculation section, and the output section.

The first section reads the model information data blocks from the UT1 file. The NASTRAN output section reads the analysis information data blocks and assigns forces and stresses to element variables, velocities to grid points, and input loads to grid points.

The power flow calculation section first calculates input powers using the input loads and corresponding grid velocities. Next, grid velocities are assigned to elements. Power flows, mechanical intensities, and power dissipations are then calculated using element forces, stresses, and the velocities of the element grids.

The output section writes power flow information on two files. The first file contains a tabular listing of the solution variables for each subcase and frequency; the second file is a data file in I-DEAS Universal file format.

Post-Processing

The user may analyze the power flow output in two ways: by inspecting the listed output, or using I-DEAS Supertab's post-processor to draw contour plots and arrow plots. Analyzing the tabular output is a good way to check power balances. Power input is equal to power dissipated plus power output. However, to visualize the entire power flow solution in any reasonably complex geometry, a good graphics post-processor is required.

Color contour plots can be used to display power flow magnitudes and power dissipations. Power flow, however, is a vector, and arrow plots are needed to display the direction of the flow. Other authors, such as Heckl,[22] and Koshiroi and Tateishi,[18] have used arrow plots to show power flows in plate structures. An alternative unavailable in I-DEAS Supertab is a combination of a contour and arrow plot, which can illustrate magnitude and direction.

TEST CASES

The test problems described here illustrate the use of beam, plate, and scalar elements. Solid elements have not been tested yet.

Simple Truss

Problem Statement

A diagram of a simple truss is shown in Fig. 5. The factor η is the assumed loss factor of the material. The truss members are constructed of three different types of cross sections. The model was attached to ground at its top and bottom by springs in all six DOF. The scalar elements simulated the effects of fasteners and the surrounding structure(s). An end force excitation was applied in all six DOF over a range of frequencies. The properties of the two W type sections are given in civil engineering handbooks.

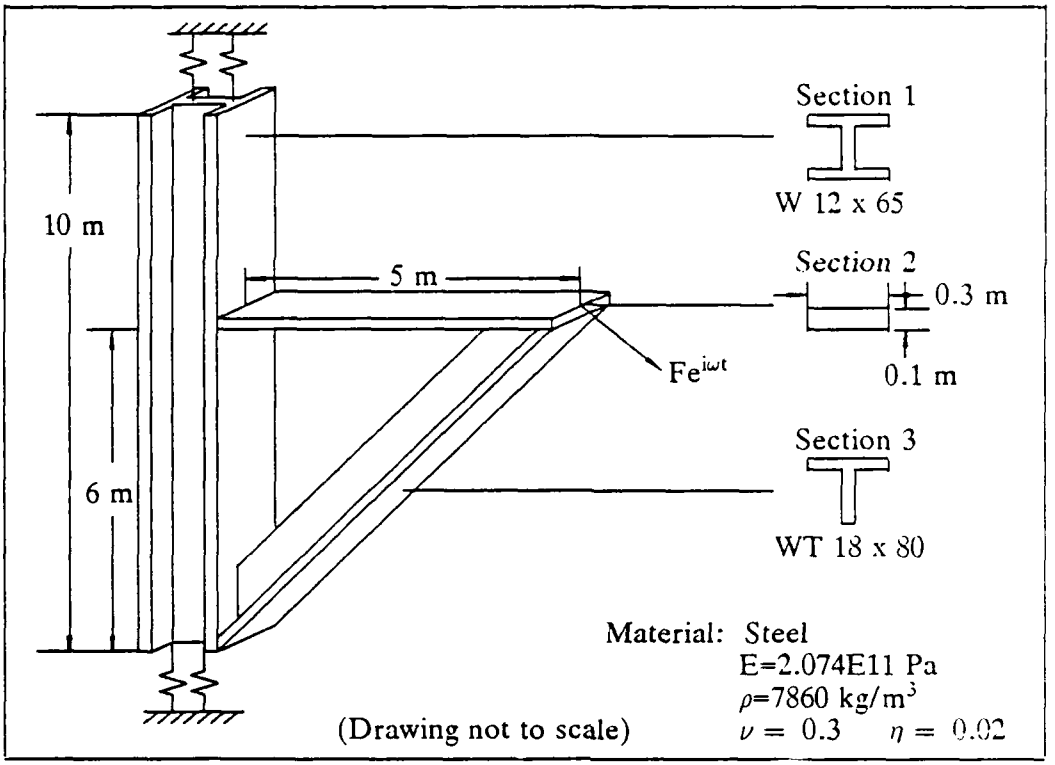

Fig. 5. Simple Truss Problem

The finite element model consisted of 74 BAR elements, with each beam section having a different mesh density. Section 1 was modeled with 40 elements of 0.25 m length, Section 2 consisted of 10 elements of 0.5 m length, and Section 3 was made up of 24 elements of about 0.325 m length. For the scalar elements, spring constants were set at about 100 to 1000 times the stiffness of the members at the appropriate DOF; the loss factor for the springs was set at 10 times the material damping constant or 0.2. This model is a good general test of the power flow methods previously outlined, since it has a varying mesh density, and the three sections have different beam properties.

Results

The first analysis performed on the model was an eigenvalue extraction (Rigid Format 3). Although there is damping in the model and the modes are actually complex, real modes may be calculated to estimate the resonances. The first 50 modes ranged in frequency from 1.87 Hz to 174 Hz. The three members experienced different types of motion in each mode (i.e., axial, flexural, or torsional), showing the need for the calculation of all types of

power flows in beams.

The end load was then applied for frequencies ranging from 1 to 100 Hz, with a resolution of 1 Hz. The plot in Fig. 6 shows the response of section three at 100 Hz, or the 29th mode of the truss. The right end of the plot is the loading point, and the left end is the junction with Section 1 and the mounting at the bottom. Both power flow and power dissipation are plotted. Power flow decreases as it propagates along the beam due to power dissipation. Power dissipation oscillates between low and high points, approximating the mode shape of the beam. When dissipation is large, power flow slopes downward; when dissipation is small, power flow remains level.

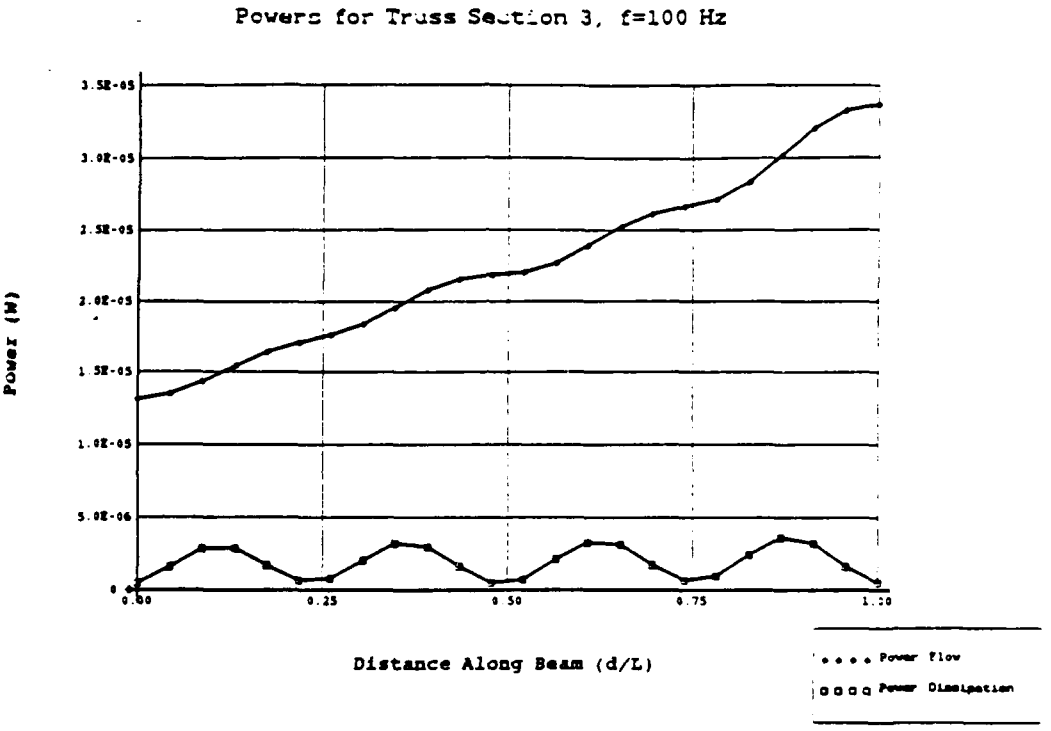

Fig. 6. Power Flows and Dissipations for a Single Frequency

Although the type of plot shown in Fig. 6 is an effective method of displaying the power flow response for a specific case, spectra plots are required to illustrate responses over the entire frequency range. The set of four plots in Figs. 7 and 8 shows power flow at different locations on each of the truss sections. Section one is split into two graphs, one is for the top half of the beam, and the other is for the bottom half.

Power flows are plotted for three locations along each member: at the beginning, middle, and end (d/L = 0.0, 0.5, and 1.0 respectively). For the top and bottom halves of Section 1, the beginning of the section is at the joint with

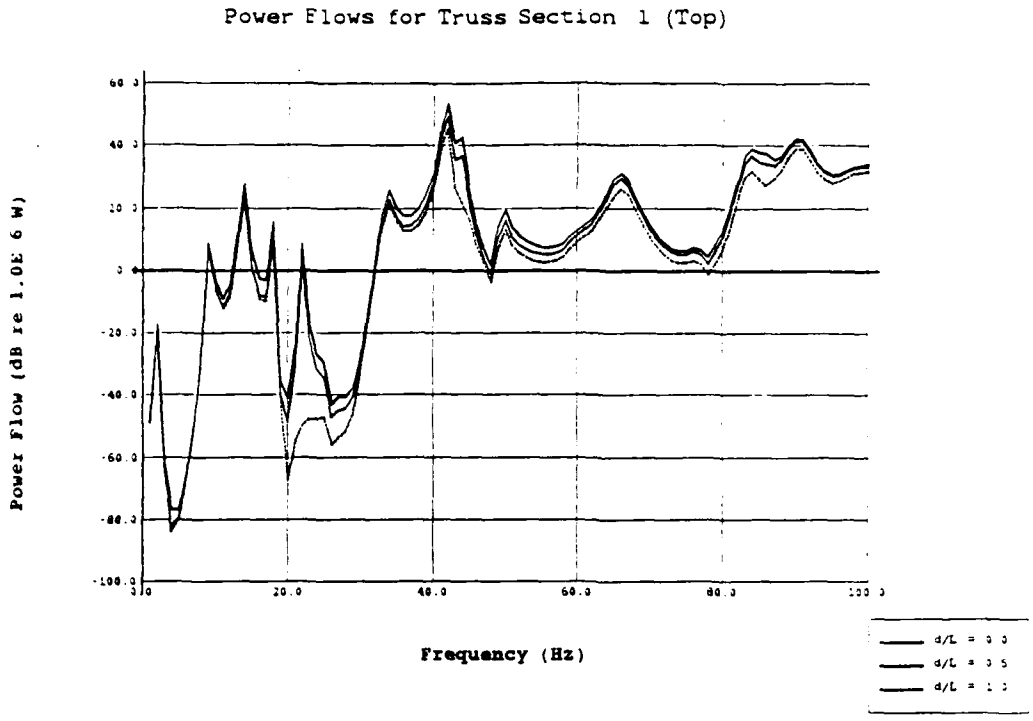

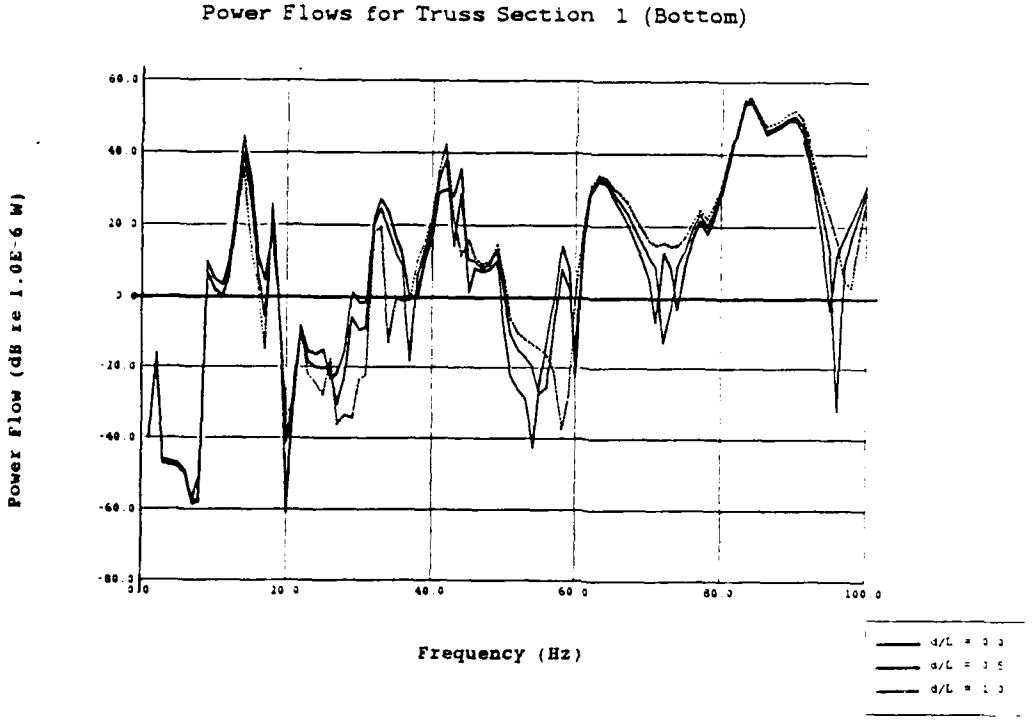

Fig. 7. Spectrum Plots of Power Flows for Truss Section 1.

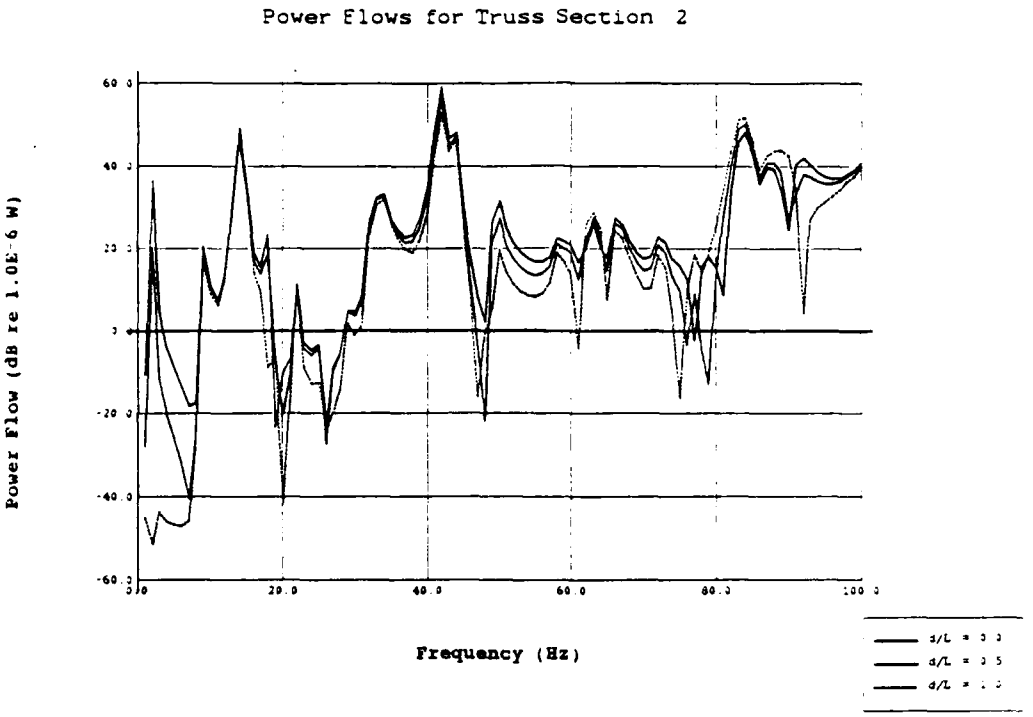

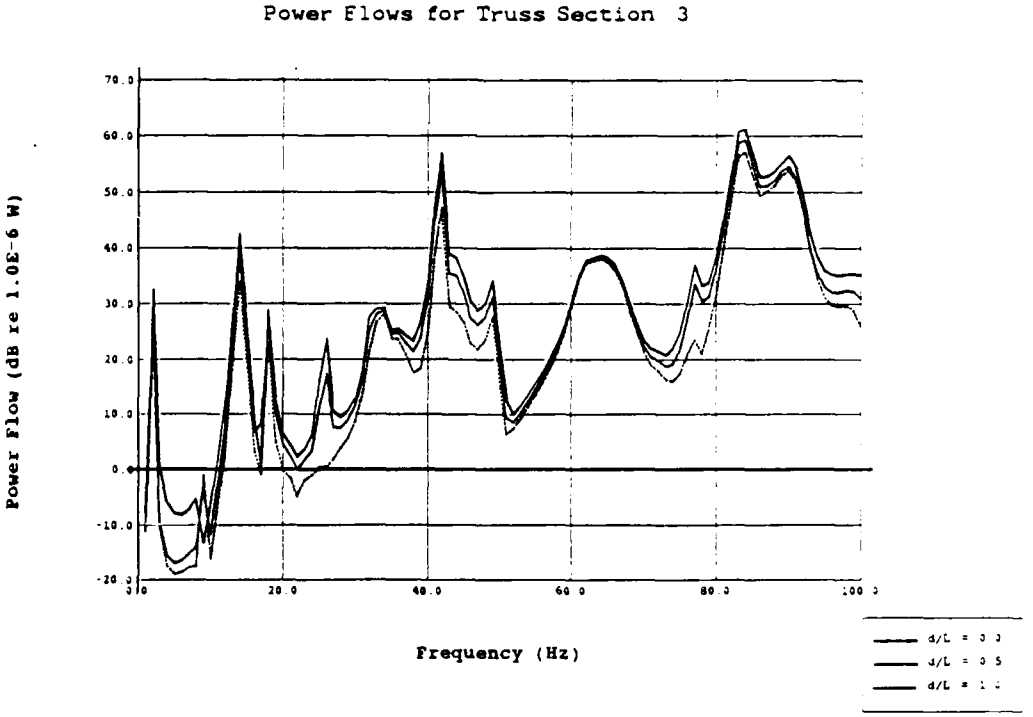

Fig. 8. Spectrum Plots of Power Flows for Truss Sections 2 and 3.

Section 2; for Sections 2 and 3, the beginning of the member is at the load point.

The expected response is a relatively uniform lowering of each curve as power flow progresses from beginning to end along each beam. This is indeed the case for some frequencies. However, at some joints, such as the junction of Sections 1 and 2 and the junction between Sections 1, 3, and ground, power flows in ways that are less intuitive. As a result, some of the plots "cross over" each other and power flow increases from beginning to end.

For different frequency bands, where different mode shapes are dominant, the nature of the power flow through the model will vary. The three power flow diagrams of Fig. 9 show some of the ways in which power may flow through the truss model in this analysis.

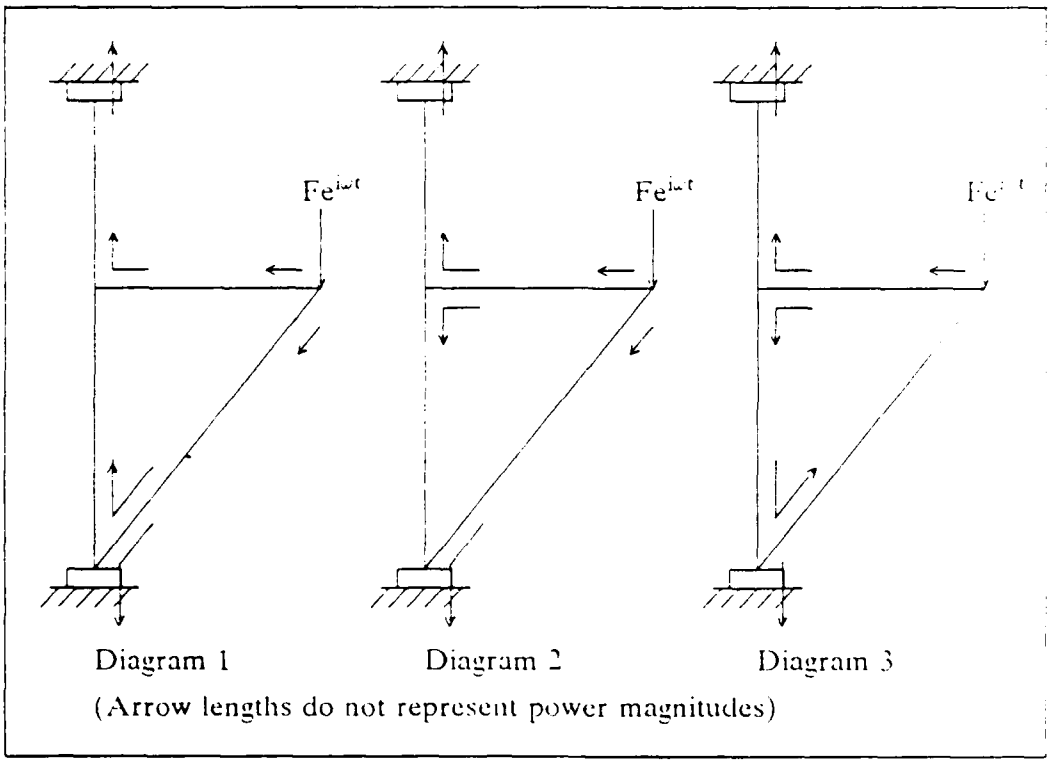

Fig. 9. Power Flow Diagrams for Truss Problem

Diagram 1 shows power entering Sections 2 and 3 at the load points and flowing out toward Section 1. At the junction of Sections 1 and 2, the power flows from Section 2 into the upper half of Section 1. At the junction of Sections 1 and 3, power flows from Section 3 into the scalar elements

connected to ground and into the bottom half of Section 1. Power then flows from the bottom of Section 1 to the top of Section 1, then up to the scalar elements at the top and out of the model.

Diagram 2 shows a similar case, but with two differences. At the junction of Sections 1 and 2, power from Section 2 flows into the top and bottom halves of Section 1; at the junction of Sections 1 and 3, power flows only into ground.

In Diagram 3, power is input only into Section 2, and flows into the top and bottom halves of Section 1. The power in the bottom half of Section 1 flows down to the junction of Section 1, Section 3, and ground, where some power flows out of the model and some flows up into Section 3.

The cases shown in Diagrams 1 and 2 are the most common as indicated by examination of the printed output. Other possibilities exist but do not occur often for the range of frequencies analyzed. The type of power flow diagram which occurs for a given frequency may be determined by examining the plots in Figs. 7 and 8. When power flow increases in going from d/L = 0.0 to d/L = 1.0, then power has entered the beam at d/L = 1.0. When power flow decreases in going from d/L = 0.0 to d/L = 1.0, then power has entered the beam at d/L = 0.0.

Response peaks in the graphs shown in Figs. 7 and 8 correspond to different types of motion in each section. Some peaks represent flexural motion, some are due to axial response, and some are torsional. A power flow algorithm which considers only flexural response would give incorrect answers to this problem.

Power balances ($P_{in} = P_{out} + \sum P_{diss}$) were accurate at the resonance frequencies where power dissipations could be calculated accurately. No power balances were performed for off-resonance frequencies since power dissipations could not be calculated accurately due to the ω_n/ω term in the calculations. Power flows at the truss joints balanced as well. A calculation based on Kirchhoff's law for currents can be made, with power flows in the BARs connected to the junctions analagous to currents.

Beam-Stiffened Cantilever Plate

The analysis of ribbed stuctures combines the power flow methods for beams and plates. Nilsson[23] used SEA methods to predict the transmission of structure-borne sound through ribbed plate models. Here, FEA is used to calculate the low frequency response of a beam-stiffened cantilever plate.

Problem Statement

A diagram of the model is shown in Fig. 10. Like the truss model, the cantilever plate model was attached to ground at its end by springs in all six DOF. The scalar elements simulated the effects of fasteners and the surrounding structure(s). A uniform end load was applied in the axial,

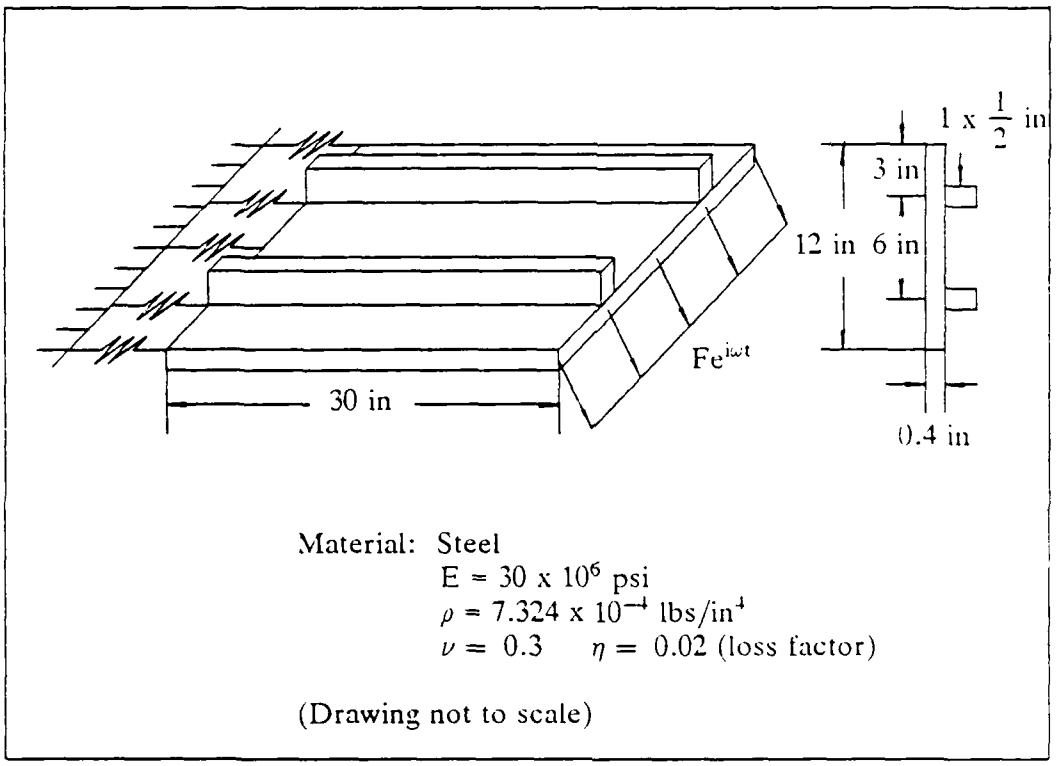

Fig. 10. Beam-Stiffened Cantilever Plate Problem

transverse shear, and bending directions. A 12 x 30 mesh of QUAD elements was used to model the plate and two sets of 30 BAR elements modeled the stiffeners. The BAR elements were offset relative to the plates. For the scalar elements, spring constants were set at about 100 to 1000 times the stiffness of the members at the appropriate DOF; the spring loss factor was set at 10 times the material damping constant or 0.2.

This model illustrates the power flow capability for plate elements and helps to test further the beam element formulation. Also, the power balance equation is checked for multiple element types in a model; the total power dissipation in the beams plus the total power dissipation in the plates must match the difference of power input and power output.

Results

An eigenvalue extraction of the model showed the first 20 natural frequencies ranging from 7.5 to 271 Hz. Loads were applied to the model for a frequency range of 5 to 250 Hz with a resolution of 5 Hz.

Fig. 11 shows a plot of input powers, summed over the loaded nodes; and output powers, summed over the scalar elements attached to the wall. The input power is approximately equal to the output power for low frequencies (less than 25 Hz). At higher frequencies power dissipation in the elements increases and the power output curve falls below the power input curve.

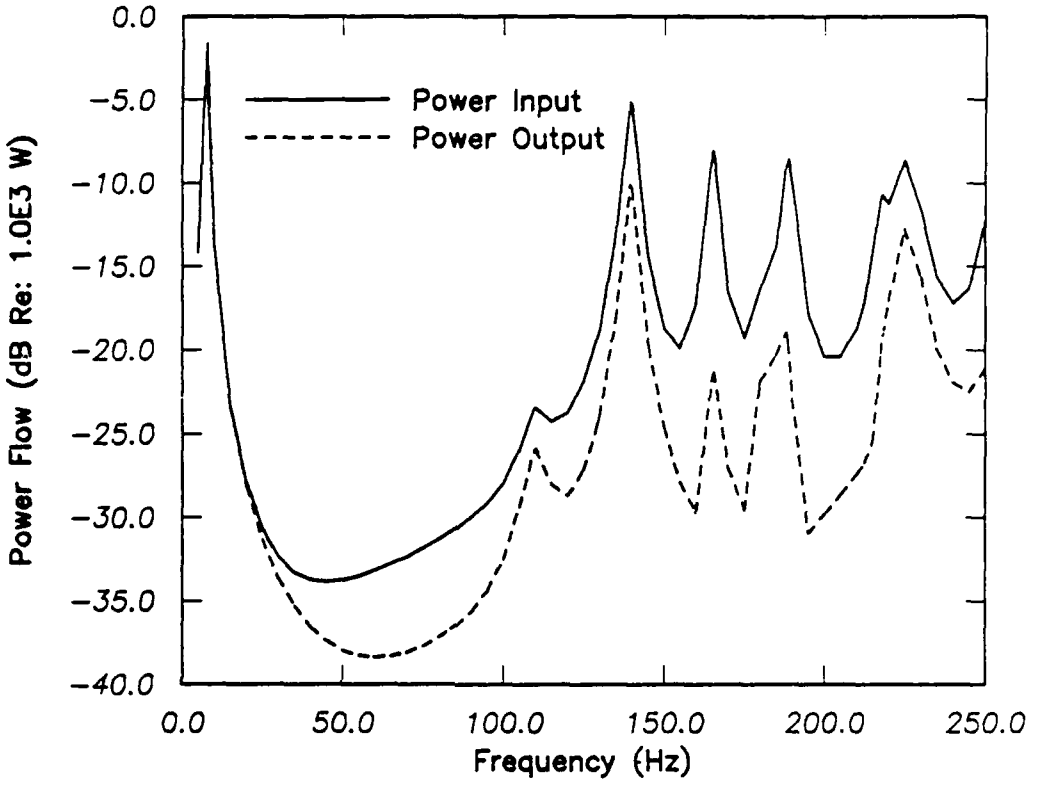

Fig. 11. Input and Output Powers for Cantilever Plate

A plot of power flows in one of the beam stiffeners over the frequency range is shown in Fig. 12. Since the model and the loading function are symmetric about the center of the plate, power flows through both beam stiffeners are the same. Curves are plotted for three locations along the beam, with d/L = 0.0 at the load point. The curves resemble those in Fig. 11, but with lower power levels. Also, the power curve at the load points is generally lower than the power curves at locations further along the beam.

To explain the behavior in the beam stiffeners, graphical (contour and vector) plots of the entire domain are needed to supplement the spectrum plots. A contour plot of the mechanical intensity magnitudes of the plate and beam elements is shown in Fig. 13, and a vector plot of mechanical intensities is in Fig. 14. Mechanical intensities are plotted rather than power flows since mechanical intensities are mesh independent for both element types. The

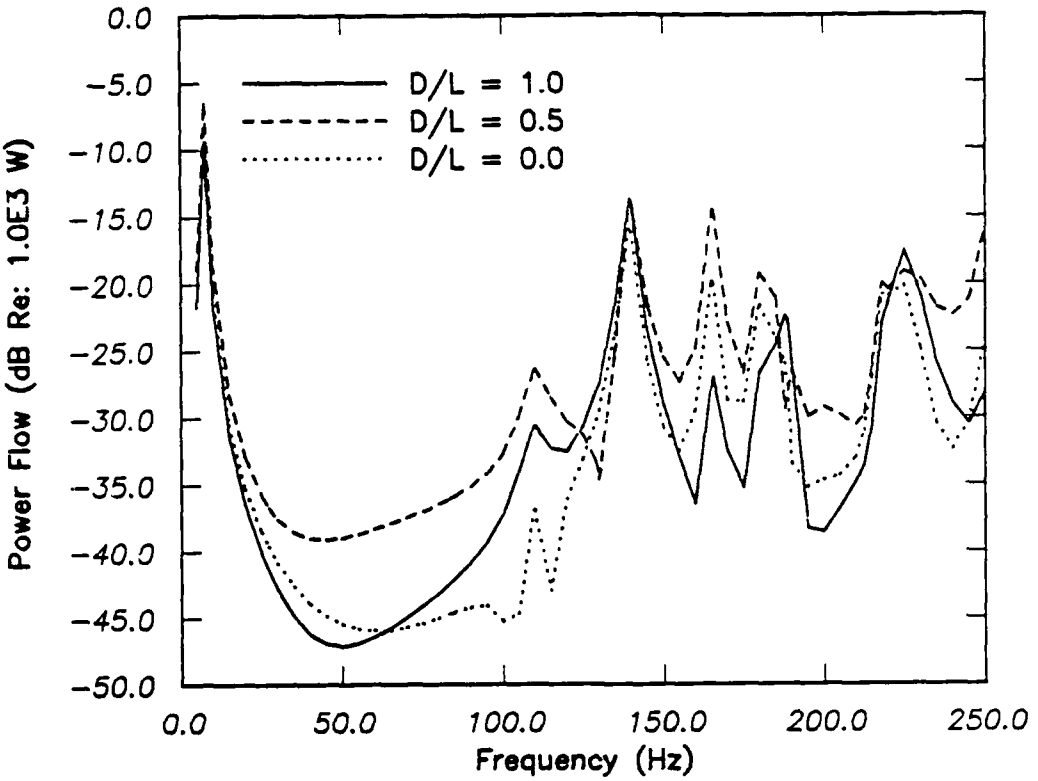

Fig. 12. Power Flows for Three Locations Along Beam Stiffener

beam elements are illustrated as plates in the diagram so their results may be visualized. Figs. 13 and 14 show how power flows through the model at 7.5 Hz (the first resonance frequency, a cantilever mode). Power flows into the model through shell elements next to the stiffeners, but is then channeled down the beams, so the power levels at beam locations further along the plate are higher than those at the load point for this frequency. About 2% of the input power is dissipated, with the rest flowing out of the model.

In this case, most of the power is flexural. At other frequencies, however, other types of power flow become dominant, such as power flow due to twisting moments and in plane membrane forces. Also, the interchange of energy between the beam stiffeners and the plate will depend on the mode shapes that are dominant for a given frequency range. This shows that the nature of a power flow field is frequency dependent. In general, no single trend can be found to explain power flow spectra over all frequencies.

The plots in Figs. 13 and 14 show the power flow field at 7.5 Hz, and explains how power flows and interchanges from plate to beam stiffener. However, other plots are needed to explain phenomena at other frequencies. With specialized graphics software being developed by Richard Van Eseltine of Code 1843 at DTRC, these plots may be animated over frequency, allowing

the analyst to observe the power flowing through a model in real time. Using such a tool, the influence of certain modes on the power flow field can be observed easily, and the nature of power flows through a given model may be better understood.

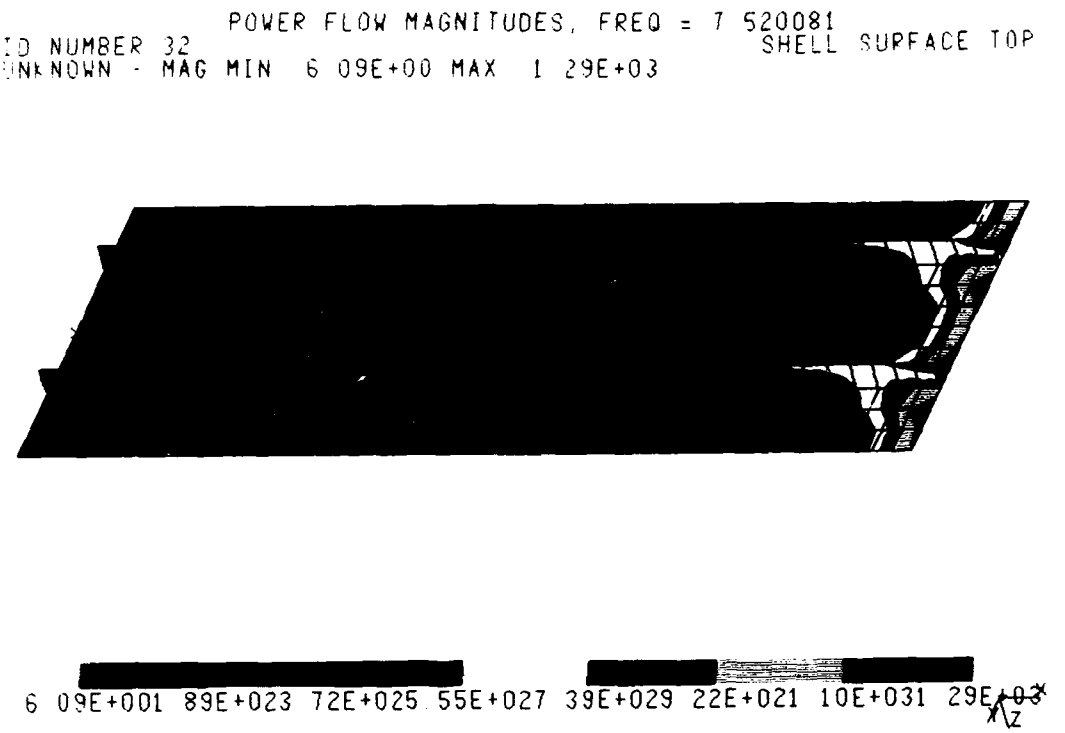

Fig. 13. Mechanical Intensity Magnitudes, f=7.55 Hz.

Power balances are accurate for resonance frequencies, with the total power dissipations of the beam and plate elements matching the differences between input and output powers. These results show that both element types may be used accurately in a single model.

SUMMARY AND FUTURE WORK

A general capability for the calculation of power flow variables (power flow, mechanical intensity, power dissipation, power input and power output) has been developed for use with the finite element code NASTRAN. BAR, QUAD2, QUAD4, HEXA2, IIHEXi, MASSi, and ELASi element types are currently supported. Unlike most of the studies described in other literature, this study considers all types of power flows - flexural, axial, and torsional - in the element formulations.

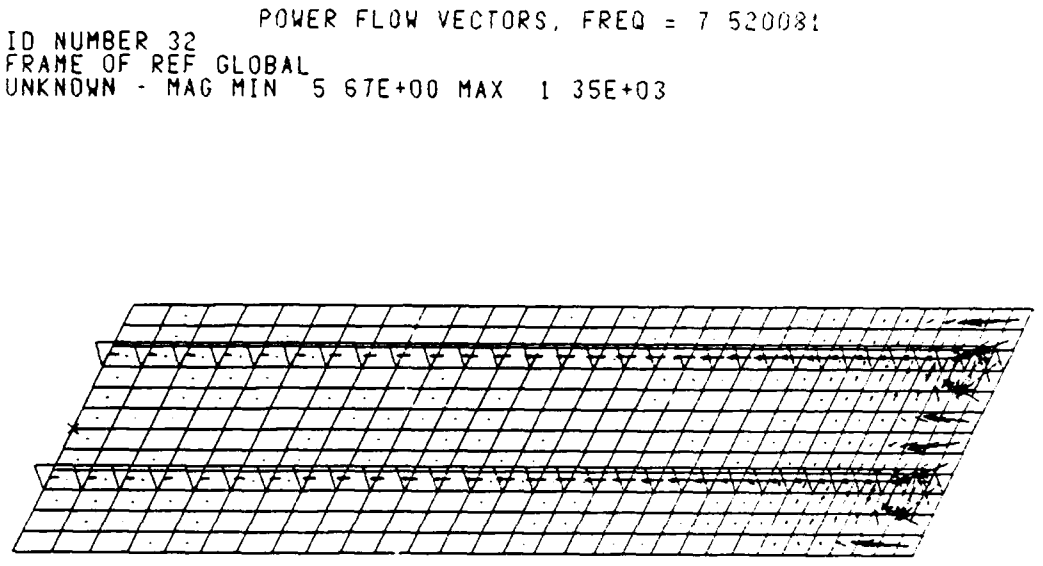

Fig. 14. Mechanical Intensity Directions f=7.55 Hz.

The results of the test problems indicate the method developed here is a valid way of predicting the power flow response of a dynamically excited system at relatively low frequencies. The results also show that the power flow paths in complex models are frequency dependent. As different modes and types of power flow become dominant, the nature of power flow fields changes. To better understand power flow fields, graphical animations of power flow contour and vector plots over frequency can be used.

The use of FEA to calculate power flows is accurate and economical for the lower modes of a mechanical system. However, the power flow results can be no better than the NASTRAN results on which they are based. Good modeling techniques and an understanding of the wavelength sizes of a problem are required. The shorter the wavelengths, the denser the required mesh will be.

Planned future work is extensive. A list of topics follows.

1. The computational methods presented here will be compared to the experimental methods developed by David Taylor of Code 274 of DTRC. Both beam and plate models will be analyzed and compared.

2. Energy is not only dissipated by material damping, but is also lost due to radiation into fluid. Ross[24] discusses the effects of entrained mass of fluid and air on the sound radiation of power. Some way of implementing the effects of entrained mass will be investigated.

3. Once power flow paths and power sinks are identified, some way of reducing P_{out} should be found. Redman-White et al.[25] and Cuschieri[26] have both discussed active force control as a means of reducing power flow. Additional forces are applied at calculated locations which alter the response of the mechanical system so that power flow is reduced. Some power sources actually act as power sinks in this case, absorbing energy from the system. This method is currently being investigated using experimental methods by John Clemens of Code 274 of DTRC. Any computational analyses will be compared to the experimental ones. Another method of reducing power flow, which has been used for many years, is the application of dampers. A few well placed dampers can absorb much of the energy in a mechanical system. A relatively new technology that could be applied to the problem is shape optimization. A given structure could be optimized for minimum sound radiation, output power, and/or weight.

APPENDIX: NASTRAN INPUT DATA

Several data blocks must be written by NASTRAN on the UT1 output file for the McPOW program. The following ALTER statements are put in the Executive Control Deck:

```
$
$ THE FOLLOWING STATEMENTS CORRESPOND TO THE 1987,88
$ VERSIONS OF COSMIC NASTRAN, RF8
$
ALTER 23$                                   AFTER THE TA1 MODULE
OUTPUT2 CASECC,EST,MPT,EQEXIN$
ALTER 135$                                  AFTER THE SDR2 MODULE
OUTPUT2 OPPC1,OESC1,OEFC1,OUPVC1,OQPC1$
ENDALTER$
```

In this alter, the CASECC data block contains case control information, the EST data block holds element information, the MPT data block contains material properties, and the EQEXIN data block holds grid and SIL (Scalar Index List) information. The OPPC1 data block contains the applied forces, the OESC1 data block lists the element stresses, the OEFC1 data block holds element forces, the OUPVC1 data block contains grid point velocities, and the OQPC1 data block contains constraint forces.

To ensure that all the required data are in the data blocks, the following output requests must be made in the case control deck:

```
FORCE=ALL
STRESS=ALL
VELOCITY=ALL
OLOAD=ALL
```

Either PHASE or REAL output data may be specified.

REFERENCES

1. Wohlever, J.C., and R.J. Bernhard, "Vibrational Power Flow Analysis of Rods and Beams," Report No. 0353-12 HL 88-24, Ray W. Herrick Laboratories, Purdue University, West Lafayette, Indiana (1988).

2. Luzzato, E., and E. Ortola, "The Characterization of Energy Flow Paths in the Study of Dynamic Systems using S.E.A. Theory," *Journal of Sound and Vibration*, Vol. 123, No. 1, pp. 189-197 (1988).

3. Rasmussen, G., "Structural Dynamic Measurements using Intensity Methods," Proceedings of the Third International Modal Analysis Conference, pp. 558-564 (1985).

4. Carroll, G., "Power Flow Measurements on a Beam with Small Localized Dampint," Proceedings of the Seventh International Modal Analysis Conference, pp. 958-964 (1989).

5. Pavic, G., "Measurement of Structure-Borne Wave Intensity, Part 1: Formulation of the Methods," *Journal of Sound and Vibration*, Vol. 49, No. 2, pp. 221-230 (1976).

6. Pinnington, E.J., "Vibrational Power Transmission to a Seating of a Vibration Isolated Motor," *Journal of Sound and Vibration*, Vol. 118, No. 3, pp.515-530 (1987).

7. Pavic, G., "Structural Surface Intensity: An Alternative Approach in Vibration Analysis and Diagnosis," *Journal of Sound and Vibration*, Vol. 115, No. 3, pp. 405-422 (1987).

8. Lyon, R.L., *Statistical Energy Analysis of Dynamical Systems*, The M.I.T. Press, (1975).

9. Mickol, J.D., and R.J. Bernhard, "An Investigation of Energy Transmission Due to Flexural Wave Propagation in Lightweight, Built-Up Structures," Report No. 0353-4 HL 86-40, Ray W. Herrick Laboratories, Purdue University, West Lafayette, Indiana (1986).

10. Cuschieri, J., "Power Flow as a Complement to Statistical Energy Analysis and Finite Element Analysis," *Statistical Energy Analysis*, ASME, NCA-Vol. 3, edited by K.H. Hsu, D.J. Nefske, and A. Adnan (1987).

11. Nefske, D.J., and S.H. Sung, "Power Flow Finite Element Analysis of Dynamic Systems: Basic Theory and Application to Beams," *Statistical Energy Analysis*, ASME, NCA-Vol. 3, edited by K.H. Hsu, D.J. Nefske, and A. Adnan (1987).

12. "NASTRAN® User's Manual, NASA SP-222(08)," Computer Software Management and Information Center (COSMIC), University of Georgia, Athens, Georgia (1986).

13. Cremer, L., M. Heckl, and E.E. Ungar, *Structure-Borne Sound*, Springer-Verlag, New York (1973).

14. Noiseux, D.U., "Measurement of Power Flow in Uniform Beams and Plates," *Journal of the Acoustical Society of America*, Vol. 47, No. 1, pp. 238-247 (1970).

15. Verheij, J.W., "Cross Spectral Density Methods for Measuring Structure-Borne Power Flow on Beams and Pipes," *Journal of Sound and Vibration*, Vol. 70, No. 1, pp. 133-139 (1980).

16. Li, J., "The Propagation of the Bending Waves and Torsional Waves in a Combined Beam Structure," Proceedings of Inter-Noise '87, pp. 611-614 (1987).

17. Williams, E.G., H.D. Dardy, and R.G. Fink, "A Technique for Measurement of Structure-Borne Intensity in Plates," *Journal of the Acoustical Society of America*, Vol. 78, No. 6, pp. 2061-2068 (1985).

18. Koshiroi, T., and S. Tateishi, "Visualization of Vibration Energy Flow in Plates: Measurements of Vibrational Intensity," Proceedings of Inter-Noise '87, pp. 1375-1378 (1987).

19. Fahy, F.J., and R. Pierri, "Application of Cross-Spectral Density to a Measurement of Vibration Power Flow Between Connected Plates," *Journal of the Acoustical Society of America*, Vol. 62, No. 5, pp. 1297-1298 (1977).

20. Cuschieri, J.M., "Extension of Vibrational Power Flow Techniques to Two-Dimensional Structures," first annual report, grant number NAG-1-685 from NASA Langley Research Center, (Aug 1987).

21. "Supertab® Engineering Analysis Pre- and Post-Processing User Guide and Reference Manual," Structural Dynamics Research Corporation, Milford, Ohio (1986).

22. Heckl, M., "Examples of Structure-Borne Sound Visualization," Proceedings of Inter-Noise '87, pp. 603-606 (1987).

23. Nilsson, A.C., "Excitation and Propagation of Structure-Borne Sound in Ribbed Structures," Proceedings of Inter-Noise '84, pp. 547-552 (1984).

24. Ross, D., *Mechanics of Underwater Noise*, Peninsula Publishing, Los Altos, California (1987).

25. Redman-White, W., Nelson, P.A., and Curtis, A.R.D., "Experiments on the Active Control of Flexural Wave Power Flow," *Journal of Sound and Vibration*, Vol. 112, No. 1, pp. 187-192 (1987).

26. Cuschieri, J.M., "Active Force Cancellation of Structure Vibrations," Proceedings of Inter-Noise '83, pp. 503-510 (1983).

INITIAL DISTRIBUTION

Copies		Copies	
17	NAVSEA	1	NORDA/Library
	1 05R		
	1 08	3	NOSC
	1 502		1 701 (H. Schenck)
	1 55N		1 733 (E. McDaid)
	1 55N (Bernhard)		1 Library
	1 55NB		
	1 55W33	4	NRL
	1 55Y		1 2312 (R. Perlut)
	1 55Y2 (R. Provencher)		1 5130 (J. Bucaro)
	1 55Y22 (D. Nichols)		1 8233 (L. Turner)
	1 55Y3 (R. Chiu)		1 Library
	1 55Y32		
	1 921N	1	NRL (Orlando)/Library
	1 PMS 393		
	1 PMS 394	3	NSWC (WO)
	1 PMS 396 (M. Bourkland)		1 R14 (H. Huang)
	1 Library		1 R31 (G. Gaunaurd)
			1 Library
1	CNO/OP-21T3 (A. Bisson)		
		1	NSWC (DL) Library
8	ONR		
	1 21 (Zimet)	6	NUSC (NL)
	1 23 (Faulstich)		1 44 (A. Carlson)
	1 23D (Fitch)		1 44 (M. Tucchio)
	1 121 (Hansen)		1 B. Sandman
	1 233 (Remmers)		1 3234 (D. Porter)
	1 1132 (Tucker)		1 3332 (D. Lee)
	1 1132 (Whitehead)		1 Library
	1 Library		
		1	NUSC (NPT)/Library
1	NADC/Library		
		1	NWC/Library
1	Naval Academy/Library		
		1	Charleston NSY/Lib
1	Naval PG School	1	Long Beach NSY/Lib
	1 M.E. Dept.	1	Mare Island NSY/Lib
	1 Library	1	Norfolk NSY/Lib
		1	Pearl Harbor NSY/Lib
1	NAVSSES (Phila.)/Library	1	Philadelphia NSY/Lib
		1	Portsmouth NSY/Lib
1	NCEL/Library	1	Puget Sound NSY/Lib
1	NCSC/Library		

Copies	
1	WPAFB (V. Venkayya)
12	DTIC
1	Alcoa Def. Systems/J. Bock
1	APL/Johns Hopkins Univ.
1	ARL/Penn State Univ.
1	AT&T Bell Labs (Whippany)/Library
2	Bettis 1 E. Zanoni 1 Library
2	Bolt, Beranek, and Newman (N. London) 1 R. Haberman 1 H. Allik
1	Butler Analyses
2	Cambridge Acoust. Assoc. 1 M. Junger 1 J. Garrelick
1	Cambridge Collaborative
1	Catholic Univ./H. Uberall
1	Colorado Univ./T. Geers
1	Donanco, Inc./D. Ross
4	General Dynamics (EB) 1 443 (J. Wilder) 1 443 (S. Gordon) 1 471 (J. Dimitri) 1 Library
1	Georgia Tech/M.E. Dept. 1 J. Ginsberg
1	J.G. Eng. Res. Assoc.

Copies	
1	JPL/M. El-Raheb
1	Lockheed Palo Alto Res. Lab/J. DeRuntz
1	Los Alamos National Lab/S. Girrens
1	Magnavox Elect. Sys./ D. Scheiber
1	Martin Marietta/Baltimore
3	Newport News Shipbuilding 1 E-12 (T. Heldreth) 1 E-92E (W. Floyd) 1 Library
3	NKF Engineering Assoc. 1 P. Kasper 1 M. Pakstys 1 R. Miller
1	Polytechnic Inst. of NY/ J. Klosner
1	Purdue University/ R.J. Bernhard
2	RPK Corporation 1 P. Pamidi 1 K. Brown
1	Tracor Applied Sciences Inc. (Cabin John)
4	Weidlinger Associates 1 M. Baron 1 J. McCormick 1 D. Ranlet 1 R. Vasudevan

CENTER DISTRIBUTION

Copies	Code		Copies	Code	
1	011		1	1844	
1	0113		1	1844	Everstine
1	0114		10	1844	Hambric
1	0117		1	185	
1	0118		1	187	
1	0119		1	189	
1	06				
			1	19	
1	12		1	1901	
1	121		1	1902	Maidanik
1	1211	Ritter	1	1904	
1	1213		1	1905.1	
			1	1905.2	
1	14		1	1905.3	
			1	1905.4	
1	15		1	1906	
1	1504		1	1908	
1	1508		1	191	
1	1522		1	192	
1	154		1	1926	Saunders
1	1542	Lee	1	193	
1	1544		1	1930.1	
			1	1930.2	
1	16		1	194	
			1	1942	
1	17		1	1942	Hwang
1	1702		1	196	
1	1703		1	1960.1	Rumerman
1	172		1	1961	
1	1720	R. Jones	1	1961	Carroll
1	1720.1		1	1961	Liu
1	1720.1	Lesar	1	1962	
1	1720.1	McNamara	1	1965	
1	1720.1	Costello			
1	173		1	27	
1	174		1	2704	
1	175		1	274	
1	177		1	2704.1	Dickey
			1	2740	Goldsmith
1	18		1	2740	Ho
1	1802		1	2742	
1	1805		1	2742	Neilson
1	182		1	2743	
1	184		1	2743	Taylor
1	1843		1	2744	

Copies	Code	
1	2749	
1	28	
1	522.1	(TIC)
1	52[illegible]	(TIC)
1	93	